Center for Turbulence Research
Proceedings of the Summer Program 1992

The evolution equation for the flame surface density in turbulent premixed combustion

By A. Trouvé[1] AND T. Poinsot[2]

One central ingredient in flamelet models for turbulent premixed combustion is the flame surface density. This quantity conveys most of the effects of the turbulence on the rate of energy release and is obtained via a modeled transport equation, called the Σ-equation. Past theoretical work has produced a rigorous approach that leads to an exact, but unclosed, formulation for the turbulent Σ-equation (Section 1.2). In this exact Σ-equation, it appears that the dynamical properties of the flame surface density are determined by a single parameter, namely the turbulent flame stretch. Unfortunately, the flame surface density and the turbulent flame stretch are not available from experiments and, in the absence of experimental data, little is known on the validity of the closure assumptions used in current flamelet models. Direct Numerical Simulation (DNS) is the obvious, complementary approach to get basic information on these fundamental quantities. In the present work, three-dimensional DNS of premixed flames in isotropic turbulent flow is used to estimate the different terms appearing in the Σ-equation (Section 2.1). A new methodology is proposed to provide the source and sink terms for the flame surface density, resolved both temporally and spatially throughout the turbulent flame brush (Section 2.2). Using this methodology, the effects of the Lewis number on the rate of production of flame surface area are described in great detail and meaningful comparisons with flamelet models can be performed (Section 3). The analysis reveals in particular the tendency of the models to overpredict flame surface dissipation as well as their inability to reproduce variations due to thermo-diffusive phenomena. Thanks to the detailed information produced by a DNS-based analysis, this type of comparison not only underscores the shortcomings of current models but also suggests ways to improve them.

1. Introduction

1.1. The flamelet approach for turbulent premixed combustion

Premixed turbulent combustion is the propagation of a chemical reaction zone through a turbulent, molecularly mixed region of fuel and oxidizer. The turbulent flame is characterized by the topology of the region in which reaction occurs: front, pockets, or large volumes. Depending on the relative values of various chemical and turbulence scales, dimensional analysis reveals a range of premixed combustion

1 Center for Turbulence Research

2 C.N.R.S., Institut de Mécanique des Fluides de Toulouse, France

modes progressing from flamelets to distributed reaction zones to well-stirred reactors (Barrère 1974, Bray 1980, Borghi 1985, Peters 1986, Williams 1985, Poinsot *et al.* 1990). These modes correspond to different topologies of the reaction zone and require different approaches for both understanding and modeling.

Experimental as well as theoretical evidence suggests that many technologically important flows occur in the flamelet burning mode. Flamelet combustion corresponds to chemical reaction occurring at fast time scales and short length scales relative to the turbulence. In this situation, the flame is confined to relatively thin layers within the turbulent flow field.

In the flamelet regime, it is convenient to describe the flame-flow interactions in terms of two basic ingredients: a flame speed that characterizes the flame structure and the flame front surface area. For instance, the mean reaction rate may be written as the product of the mean fuel consumption rate per unit flame surface area times the flame surface density:

$$\langle \dot{\omega}_R \rangle = (\rho_u Y_{R,u} \langle S_C \rangle_S) \, \langle \Sigma' \rangle, \tag{1}$$

where $\dot{\omega}_R$ is the mass of fuel consumed per unit time and per unit volume; ρ_u and $Y_{R,u}$ are respectively the density and the fuel mass fraction in the unburnt gas; S_C is the local integral of the reaction rate along the flame normal direction, $S_C = \int \dot{\omega}_R dn$, and characterizes the local combustion intensity; and Σ' is the flame surface area per unit volume. The flame surface density is defined as the expected value for Σ': $\Sigma = \langle \Sigma' \rangle$.

In Eq.(1), the flamelet speed, $\langle S_C \rangle_S$, accounts for local variations of the reaction rate along the flame surface. Laminar flame theory indicates that the local flame structure is modified by flow divergence, usually characterized by the hydrodynamic strain rate acting in the flame tangent plane as well as by flame front curvature. Under certain conditions, these variations can become critical and lead to partial or total quenching of the flame. Recent studies, however, using Direct Numerical Simulations (DNS) suggest that quenching is a rather unlikely event for turbulent premixed flames (Poinsot *et al.* 1990). In addition, although the local combustion intensity may exhibit large variations along the turbulent flame front, particularly for non-unity Lewis number flames, DNS suggest that these variations always tend to cancel in the mean (Haworth & Poinsot 1992, Rutland & Trouvé 1991). In the simulations, the mean fuel consumption speed, $\overline{S}_C$, defined as the area-weighted, space-averaged value of S_C integrated along the turbulent flame surface, remain within 10% to 30% from the one-dimensional, laminar flame speed value, s_L.†

Thus, it appears that in the absence of quenching, the mean fuel consumption speed, $\overline{S}_C$, is only weakly sensitive to the flow field and the principle effect of turbulence is for the fluctuating velocity field to wrinkle the flame and greatly increase its surface area. This phenomenon accounts for most of the increase in the

† Note that $\overline{S}_C$ is a space-averaged quantity and should not be confused with $\langle S_C \rangle_S$ which is an area-weighted ensemble-average as defined in section 1.2 and, therefore, depends on location within the turbulent flame brush (see Figure 7)

overall burning rate due to the turbulence and is represented in Eq.(1) through the flame surface density, Σ.

1.2. The evolution equation for the flame surface density, Σ

In current flamelet models, the flame surface density, Σ, is obtained via a modeled transport equation. This equation was first postulated by Marble & Broadwell (1977) based on phenomenological grounds. A more rigorous approach was later proposed by Pope (1988) and Candel & Poinsot (1990) who derive an exact balance equation for the flame surface-to-volume ratio, Σ':

$$\frac{\partial \Sigma'}{\partial t} + \nabla.\dot{\mathbf{X}}\Sigma' = (\nabla.\dot{\mathbf{X}} - \mathbf{nn} : \nabla\dot{\mathbf{X}})\ \Sigma', \tag{2}$$

where $\dot{\mathbf{X}}$ is the displacement speed of the flame surface, given by the sum of the fluid velocity and the flame propagation speed in the normal direction: $\dot{\mathbf{X}} = \mathbf{u} + w\mathbf{n}$; $\mathbf{n}$ is the unit vector normal to the flame surface; and where we use tensorial notations: $(\mathbf{nn} : \nabla\dot{\mathbf{X}}) = n_i n_j \frac{\partial \dot{X}_i}{\partial x_j}$.

The right-hand side of Eq.(2) can also be expressed in terms of flame stretch. The flame stretch, k, is defined as the rate of change of a Lagrangian flame surface element, δA:

$$k = \frac{d(\delta A)}{dt} = \frac{\partial(\delta A)}{\partial t} + \dot{\mathbf{X}}.\nabla(\delta A) \tag{3}$$

A more useful expression for k is in terms of strain rate, flame curvature, and flame propagation speed (see for example Candel & Poinsot 1990):

$$k = a_T + 2wk_m, \tag{4}$$

where a_T is the rate of strain acting in the flame tangent plane: $a_T = \nabla.\mathbf{u} - \mathbf{nn} : \nabla\mathbf{u}$; and k_m is the flame surface curvature, as given by the divergence of the flame normal direction: $2k_m = \nabla.\mathbf{n}$. In Eq.(4), positive curvature is chosen convex towards the reactants.

Using Eq.(4), the balance equation for the flame surface-to-volume ratio can be re-written as:

$$\frac{\partial \Sigma'}{\partial t} + \nabla.\dot{\mathbf{X}}\Sigma' = k\ \Sigma' \tag{5}$$

When ensemble-averaged, this equation yields an exact balance equation for the flame surface density (Pope 1988, Cant *et al.* 1990):

$$\frac{\partial \Sigma}{\partial t} + \nabla.\langle\dot{\mathbf{X}}\rangle_S \Sigma = \langle k\rangle_S\ \Sigma, \tag{6}$$

where the flame surface mean of any quantity Q is given by: $\langle Q\rangle_S = \langle Q\Sigma'\rangle/\langle\Sigma'\rangle = \langle Q\Sigma'\rangle/\Sigma$. Note that surface means are different from standard means; in particular, the surface mean of a quantity Q is different from the ensemble mean of Q conditioned on being at the flame location (see section 2.2).

Eq.(6) can be cast in various forms. For modeling purposes, it is useful to split the velocity vector into a mean component and a turbulent fluctuation: $\mathbf{u} = \langle \mathbf{U} \rangle + \mathbf{u}'$. We can then re-write Eq.(6) as follows:

$$\frac{\partial \Sigma}{\partial t} + \nabla.\langle \mathbf{U} \rangle \Sigma + \nabla.\langle \mathbf{u}' \rangle_S \Sigma + \nabla.\langle w\mathbf{n} \rangle_S \Sigma = \langle a_T \rangle_S \, \Sigma + \langle A_T \rangle_S \, \Sigma + 2\langle w k_m \rangle_S \, \Sigma, \quad (7)$$

where we use the following notations:

$$\langle a_T \rangle_S = \langle \nabla.\mathbf{u}' - \mathbf{nn} : \nabla \mathbf{u}' \rangle_S,$$
$$\langle A_T \rangle_S = \nabla \langle \mathbf{U} \rangle - \langle \mathbf{nn} \rangle_S : \nabla \langle \mathbf{U} \rangle$$

The three convective terms on the left-hand side of Eq.(7) are transport terms that correspond respectively to convection by the mean flow, turbulent diffusion, and flame propagation. The terms on the right-hand side of the equation are the source and sink terms for the flame surface density: $\langle a_T \rangle_S$ is the turbulent strain rate acting in the flame tangent plane, $\langle A_T \rangle_S$ is the strain rate due to the mean flow field, and $2\langle w k_m \rangle_S$ is a term that accounts for the combined effects of flame curvature and flame propagation.

The principle effect of turbulence is to increase the flame surface area, and $\langle a_T \rangle_S$ is without ambiguity a source term in the equation for Σ. The effect of the mean flow field as measured by $\langle A_T \rangle_S$ is problem dependent; depending on the flow configuration, its sign can be positive or negative. We now focus attention on the last term in Eq.(7), referred to as the propagation term.

In many situations, flame propagation effects merely counteract the wrinkling due to the turbulence and the propagation term, $2\langle w k_m \rangle_S$, is, therefore, expected to be negative. Consequently, this term is usually described as a sink term in flamelet models. There are some situations, however, where this description is clearly incorrect. Since the propagation term includes some of the effects associated with intrinsic flame instabilities†, this term must depend on the flame properties, thereby allowing for situations where its sign is positive and where the net effect corresponds to a production of flame surface.

The exact importance of laminar flame instabilities for turbulent combustion is an open subject. Recent evidence, however, both experimental (Abdel-Gayed *et al.* 1984, Wu *et al.* 1990, Goix & Sheperd 1992) and numerical (Ashurst *et al.* 1987, Haworth & Poinsot 1992, Rutland & Trouvé 1991), suggests that the role of the Lewis number has been underestimated in the past. For instance, current flamelet models fail to account for the effects of the Lewis number on the rate of production of flame surface. The objective of the present study is to determine how present formulations might be improved to incorporate such effects. The approach is to analyze the source and sink terms in the equation for the flame surface density, with particular emphasis on how the Lewis number can affect their balance. This is accomplished using DNS, as described in the next section.

† Using the terminology introduced to describe laminar flame instabilities, the propagation term represents the thermo-diffusive mechanism, while the strain term represents the hydrodynamic mechanism. These two instability mechanisms are coupled together and both account for Lewis number effects (Clavin 1985, Williams 1985)

2. Direct Numerical Simulation of turbulent premixed flames

2.1. Numerical method and configuration

We use DNS to analyze the different terms appearing in the equation for the flame surface density. The simulations are performed using a three-dimensional, compressible Navier-Stokes solver that fully resolves the turbulent flow field. Spatial derivatives are computed with a modified Padé scheme that is sixth-order accurate (Lele 1990). Solutions are advanced in time using a third-order Runge-Kutta method (Wray 1990). Boundary conditions are specified using the NSCBC method (Poinsot & Lele 1992). Because of the otherwise prohibitive computational cost, simulations are limited to simple but finite-rate reaction schemes. In this work, the chemistry model is a single step, irreversible chemical reaction where the reaction rate depends exponentially on temperature (Arrhenius kinetics):

$$\dot{\omega}_R = B\rho Y_R \exp\left(-\frac{T_a}{T}\right), \tag{8}$$

where T_a is the activation temperature and B is a constant that depends on the flame speed. This formulation corresponds to a binary reaction in which one of the reactants, Y_R, is strongly deficient as, for example, in fuel-lean combustion. Also, it is worth emphasizing that the simulations are not limited by the constant density assumption, and heat release effects are fully accounted for.

Following Williams (1985), we re-write the reaction rate as:

$$\dot{\omega}_R = \Lambda\rho Y_R \exp\left(\frac{-\beta(1-\Theta)}{1-\alpha(1-\Theta)}\right), \tag{9}$$

where Θ is the reduced temperature, $\Theta = (T-T_u)/(T_b-T_u)$; T_u is the temperature of the fresh reactants; T_b is the adiabatic flame temperature; and the coefficients Λ, α, and β are, respectively, the reduced pre-exponential factor, the heat release factor, and the reduced activation energy:

$$\Lambda = B\exp(-\beta/\alpha), \quad \alpha = (T_b - T_u)/T_b, \quad \text{and} \quad \beta = \alpha T_a/T_b \tag{10}$$

In the following, we use $\alpha = 0.75$ and $\beta = 8$.

Another important feature of the simulations is that transport coefficients are temperature dependent. These coefficients satisfy the following relations:

$$\mu = \mu_u(T/T_u)^b\ ,\ Le = \lambda/\rho D c_p = \text{constant}\ ,\ Pr = \mu c_p/\lambda = \text{constant}\ , \tag{11}$$

where μ, λ, and D are the molecular diffusivities of, respectively, momentum, internal energy, and species mass, b is a constant, and Le and Pr are respectively the Lewis number and the Prandtl number. We use $b = 0.76$, $Pr = 0.75$. Simulations have been performed for different Lewis numbers, $Le = 0.8, 1.0$, and 1.2.

The selected computational configuration corresponds to a premixed flame embedded in three-dimensional, decaying, isotropic turbulent flow. The left- and right-hand sides of the computational domain are inflow and outflow boundaries while

periodic boundary conditions are applied at lateral walls. The calculations are initialized with fresh reactants on one side of the domain and burnt products on the other side; the two are separated by a plane laminar flame. Isotropic turbulence is initially located in the flow of fresh reactants, its velocity field being specified according to a model spectrum. The turbulence is characterized by a Kolmogorov length scale smaller than the thermal thickness of the laminar flame, $\eta_k/\delta_T = 0.1$ where $\delta_T = (T_b - T_u)/(dT/dx)_{max}$, and a turbulence intensity that is much higher than the laminar flame speed, $u'/s_L = 10$. The initial turbulent Reynolds number, based on the Taylor microscale, is 50. The initial turbulent Reynolds number, based on the integral length scale, is 70. The grid resolution is 129^3.

The simulations describe the wrinkling of the flame zone due to turbulent motions as well as the combustion feedback due to dilatation and temperature-dependent transport properties. Note that the turbulence is decaying in time, and conditions are non-stationary.

2.2. Diagnostics

All terms appearing in Eq.(7) may be obtained from the simulations. We now briefly describe how. The velocity vector and the velocity gradient tensor are readily obtained from the resolved flow field. To define flame-based quantities, we make use of concepts based on a thin flame picture. First, a progress variable, c, is introduced that is used to indicate location within the reaction zone, $c = 1 - Y_R$, where Y_R is the normalized fuel mass fraction. The progress variable varies monotonically through the flame from 0 in the reactants to 1 in the products. Constant progress variable surfaces may conveniently be used to define the flame front location: we use the surface $c = c_f = 0.8$. In addition, at any location on this surface, the local gradient of c defines the normal direction to the flame front:

$$\mathbf{n} = -\frac{\nabla c}{|\nabla c|}, \tag{12}$$

where $\mathbf{n}$ points into the fresh reactants.

The propagation speed of the flame surface, w, is obtained from an expression analog to the well-known field equation (also called the G-equation). Let us first consider a point on the flame surface, $c = c_f$. The velocity, $\dot{\mathbf{X}}$, at which this point must move to remain on the surface is given by:

$$\frac{\partial c}{\partial t} + \dot{\mathbf{X}}.\nabla c = 0, \tag{13}$$

which, using Eq.(12), implies that:

$$\dot{\mathbf{X}}.\mathbf{n} = \frac{1}{|\nabla c|}\frac{\partial c}{\partial t}, \tag{14}$$

and which yields the following expression for the flame propagation speed:

$$w = \dot{\mathbf{X}}.\mathbf{n} - \mathbf{u}.\mathbf{n} = \frac{1}{|\nabla c|}\frac{Dc}{Dt}, \tag{15}$$

where quantities are estimated at the surface $c = c_f$. Since in the simulations we solve for a conservation equation for the fuel mass fraction, Y_R, and since by definition $c = 1 - Y_R$, the expression above can be readily obtained from the DNS data base.

The flame surface density, Σ, is a more subtle quantity. It includes both geometrical and statistical information. Following Pope (1990), the flame surface density is computed as the product of the expected value for the magnitude of the gradient of c, conditioned on being on the flame surface, times the probability of being on that surface:

$$\Sigma' = |\nabla c| \ \delta(c - c_f), \quad \text{and} \quad \Sigma = \langle \Sigma' \rangle = \langle |\nabla c| \mid c = c_f \rangle \ p(c_f), \tag{16}$$

where $p(c_f)$ is the probability of $c = c_f$.

We now turn to the averaging problem. In the simulations, the flame brush propagates along the x direction, and the problem remains homogeneous in the $y - z$ planes. Therefore, averaged quantities depend on x and time t only, and ensemble-averaging can be performed in the $y - z$ planes:

$$\langle Q \rangle(x,t) = \frac{1}{L_y L_z} \int Q(x,y,z,t) dy dz, \tag{17}$$

where L_y and L_z are the y and z dimensions of the computation domain. The accuracy of this expression depends on the size of the computational domain with respect to the turbulent length scales. In the simulations, the integral length scale of the turbulent flow field grows as the kinetic energy decays; this growth, however, is rather slow, and it was determined that the integral length scale remains at least 8 times smaller than L_y and L_z. Typically, in every $y - z$ plane within the turbulent flame brush, the statistical sample consists of approximately 10 fully independent flame events, and, although we recognize that the statistics are somewhat undersampled, reasonable accuracy is expected when estimating the first moments.

Conditional means are computed by integrating along the $c = c_f$ contour:

$$\langle Q \mid c = c_f \rangle(x,t) = \frac{\int_{c=c_f} Q \ dl}{\int_{c=c_f} dl} \tag{18}$$

Surface means are then obtained using the following relations:

$$\langle Q \rangle_S(x,t) = \frac{\langle Q\Sigma' \rangle}{\langle \Sigma' \rangle} = \frac{\langle Q|\nabla c| \mid c = c_f \rangle}{\langle |\nabla c| \mid c = c_f \rangle} = \frac{\int_{c=c_f} Q|\nabla c| \ dl}{\int_{c=c_f} |\nabla c| \ dl} \tag{19}$$

Clearly, surface means differ from conditional means.

The relations above provide a methodology to estimate the different means needed in our analysis. As shown in Eq.(16), the flame surface density, Σ, also requires

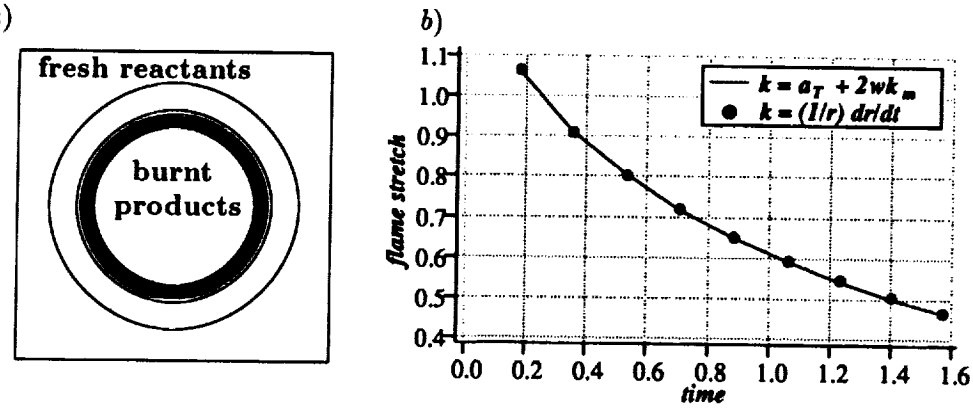

FIGURE 1. A test case for flame stretch: the problem of a cylindrical, freely-expanding, premixed laminar flame: a) temperature contours; b) flame stretch: solid line based on Eq.(4); symbols based on Eq.(22).

an estimate of the probability $p(c_f)$. Simple geometrical considerations lead to the following relation:

$$p(c_f) = \frac{1}{L_y L_z} \int_{c=c_f} \frac{dl}{\sqrt{(\frac{\partial c}{\partial y})^2 + (\frac{\partial c}{\partial z})^2}}, \tag{20}$$

and finally, Eqs.(16), (18) and (20) yield the following expression for Σ:

$$\Sigma = \frac{1}{L_y L_z} \int_{c=c_f} \frac{dl}{\sqrt{(\frac{\partial c}{\partial y})^2 + (\frac{\partial c}{\partial z})^2}} \frac{\int_{c=c_f} |\nabla c| \, dl}{\int_{c=c_f} dl} \tag{21}$$

Before applying these diagnostics to the turbulent flame simulations, we check the accuracy of our estimates for flame stretch and flame propagation speed using a model laminar flame problem as described in the next section.

2.3. Validation of DNS-based estimates for flame stretch

As seen in Eqs.(5) and (6), the flame stretch, k, is the single relevant parameter that determines the growth rate of flame surface area. Since this growth rate is locally exponential, it is important to obtain accurate estimates for k. In our analysis, the flame stretch is obtained using Eq.(4). The overall accuracy of our analysis thus depends on our ability to predict correctly strain rate, flame curvature, and flame propagation speed. To check the accuracy of our estimates, we performed simulations of a cylindrical, premixed laminar flame expanding freely into an initially quiescent medium (Figure 1a). In this model problem, the flame stretch can be directly measured from the growth of the flame radius:

$$k = \frac{1}{r_f} \frac{dr_f}{dt}, \tag{22}$$

where r_f designates the radius of the flame contour, $c = c_f$. Results based on this expression are compared with our DNS-based estimates in Figure 1b. The very

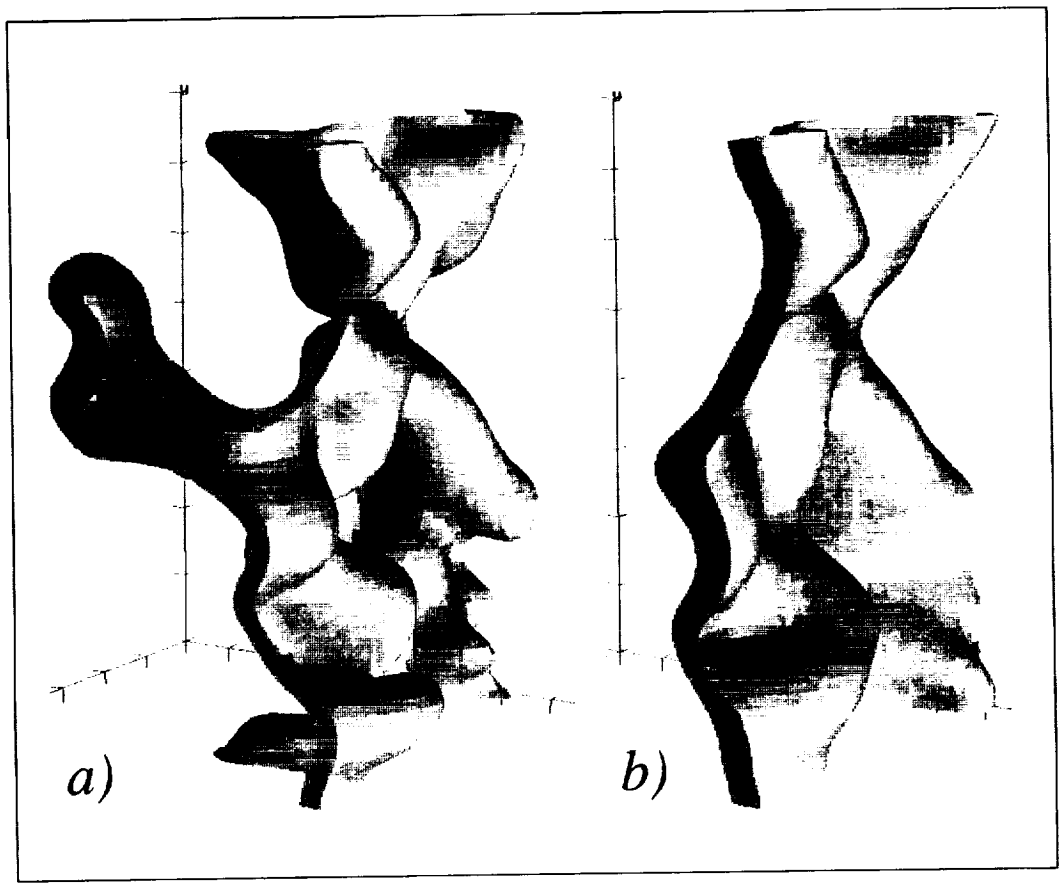

FIGURE 2. DNS of turbulent premixed flames in isotropic flow. Snapshots of the flame surface after 3.5 turbulent eddy turn-over time: a) $Le = 0.8$; b) $Le = 1.2$. The flow is from top-left (reactants) to bottom-right (products).

good agreement seen in Figure 1b demonstrates that the flame stretch as well as the flame propagation speed can be accurately monitored with our diagnostics.

3. Results and discussion

As described in the previous section, the present study uses three-dimensional, direct numerical simulations of turbulent premixed flames in isotropic flow. Three different cases have been studied that correspond to turbulent flames characterized by the same laminar thermal thickness, δ_T, the same laminar flame speed, s_L, embedded in the same initial turbulent flow field, but with different Lewis number, $Le = 0.8$, 1.0 and 1.2 (Figure 2).

3.1. The overall effect of the Lewis number

Figure 3 shows that the three cases exhibit large differences in the time history of the total reaction rate (space-averaged over the computational domain). After 4 turbulent eddy turn-over time, $t = 4\tau$, the $Le = 0.8$ flame burns more than twice as

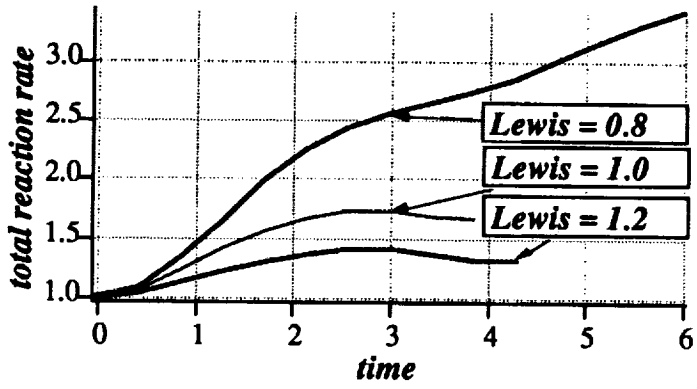

FIGURE 3. Lewis number effects on the overall combustion intensity. The total reaction rate is made non-dimensional by its initial value corresponding to a strain-free, plane laminar flame. Time is made non-dimensional by the initial, turbulent eddy turn-over time, τ.

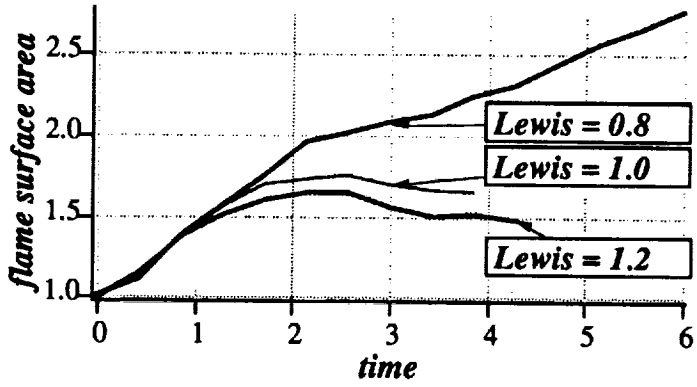

FIGURE 4. Lewis number effects on the relative increase of total flame surface area. Time is made non-dimensional by the turbulent eddy turn-over time, τ.

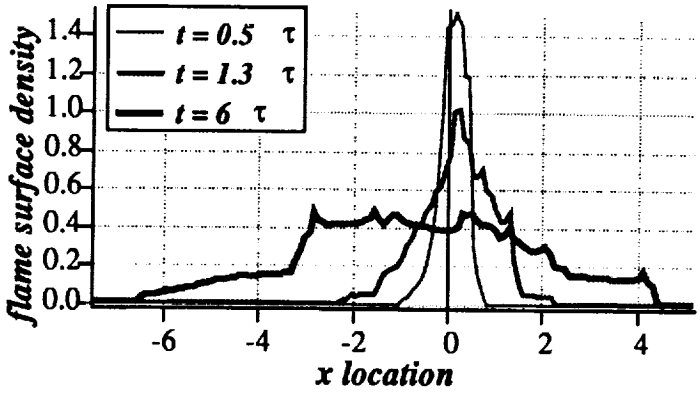

FIGURE 5. Time evolution of the flame surface density, Σ, through the turbulent flame brush (reactants on the left; products on the right). $Le = 0.8$. Σ and x are made non-dimensional by the laminar thermal thickness, δ_T. Time is measured in units of the turbulent eddy turn-over time, τ.

much as the $Le = 1.2$ flame. In agreement with the findings from previous studies (Ashurst *et al.* 1987, Haworth & Poinsot 1992, Rutland & Trouvé 1991), the mean fuel consumption speed, $\overline{S}_C$, irrespective of the value of the Lewis number, is found to be only a weak function of the turbulence: at all times, departures of $\overline{S}_C$ from the laminar value, s_L, remain within 20%. Thus, the principal effect of the Lewis number is to promote or inhibit the production of flame surface area.

The drastic effect of the Lewis number on flame surface production is displayed in Figure 4. For $Le = 1.0$ and $Le = 1.2$, the flame surface area initially increases, reaches a maximum, and then decreases in time. The increase occurs as the turbulence wrinkles the initially flat flame surface. The flame then adapts to its turbulent environment, and, as the turbulence decays, the flame surface becomes smoother and relaxes to its initial state. The $Le = 0.8$ flame exhibits a strikingly different behavior: the flame surface area keeps increasing in time without saturation. Although saturation might be expected at later times, our simulations are limited by the size of the computational domain and this subsequent phase cannot be observed. In any case, the simulations indicate that saturation will not occur on a time scale characteristic of the turbulence, and, in that sense, the flame can be said to be unstable.

The differences between the $Le = 0.8$ and $Le = 1.2$ flames are in fact so pronounced that they can easily be observed by comparing instantaneous snapshots of the flame surface (Figure 2). For instance, for $Le = 0.8$, fingers of burnt products are seen to propagate at a fast rate into the fresh reactants (Figure 2a). We believe this "fingering" is an important ingredient of the flame instability process. The "fingering" is not observed in the $Le = 1.0$ or $Le = 1.2$ flames (Figure 2b).

3.2. The source and sink terms in the equation for Σ

The effects of the Lewis number are now further studied by analyzing the structure of the terms appearing on the right-hand side of the equation for the flame surface density, Σ. As described in section 2.2, the analysis takes advantage of the fact that the problem is statistically one-dimensional and provides the source and sink terms for Σ as a function of time t and position x within the turbulent flame brush.

Figure 5 compares several Σ-profiles through the turbulent flame brush taken at different instants in the simulations. The Lewis number is 0.8. At $t = 0$, Σ is a delta function located at $x = 0$. As time evolves, the turbulent flame brush gets thicker and propagates deeper into the reactants. Accordingly, the Σ-profile spreads out and shifts towards negative values of x. In the simulations, this shift is rather weak but can clearly be seen at the latest times ($t = 6\tau$ in Figure 5). Note that the integral of Σ through the flame brush gives the relative increase of total flame surface area:

$$\int \Sigma(x,t)\, dx = \frac{S_V(t)}{L_y L_z}, \tag{23}$$

where $S_V(t)$ is the flame surface area within the computational domain of size V.

The main advantage of the present analysis is to distinguish between the leading edge and the rear edge of the turbulent flame brush. The geometry as well as the dynamics of the flame differ quite significantly from one end of the reaction zone

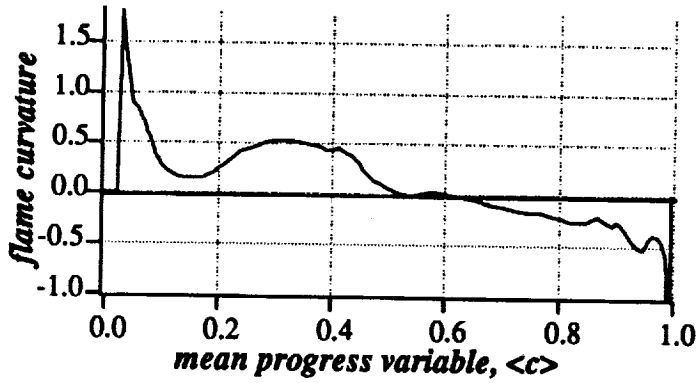

FIGURE 6. Variations of the mean flame curvature, $\langle k_m \rangle_S$, through the turbulent flame brush. $Le = 0.8$, $t = 4\ \tau$. Flame curvature is made non-dimensional by the laminar thermal thickness, δ_T.

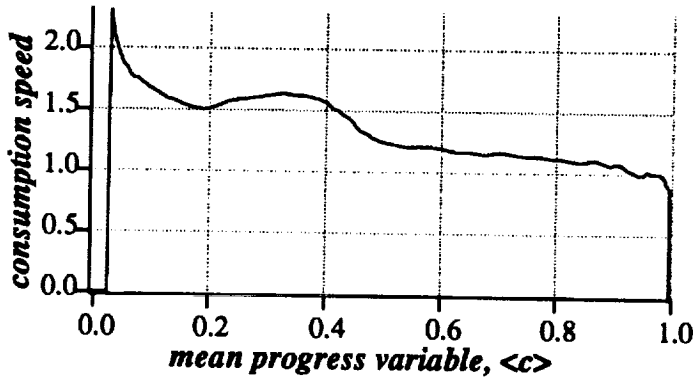

FIGURE 7. Variations of the mean fuel consumption speed, $\langle S_C \rangle_S$, through the turbulent flame brush. $Le = 0.8$, $t = 4\ \tau$. S_C is made non-dimensional by the laminar flame speed, s_L.

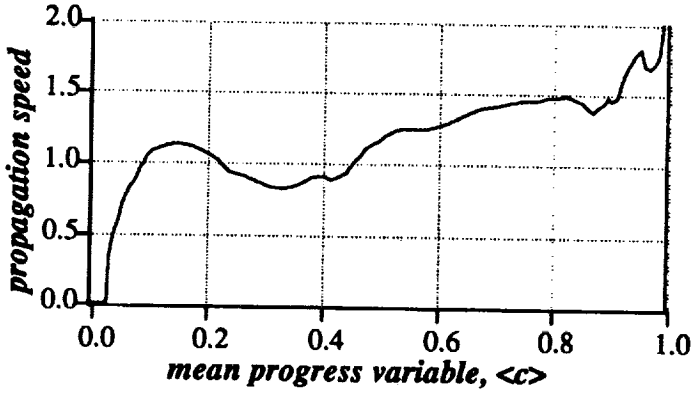

FIGURE 8. Variations of the mean flame propagation speed, $\langle w \rangle_S$, through the turbulent flame brush. $Le = 0.8$, $t = 4\ \tau$. w is made non-dimensional by its value corresponding to a strain-free, plane laminar flame, $w = s_L \rho(c = 0)/\rho(c = c_f)$.

to the other as shown in Figures 6 to 12. For convenience, in Figures 6 to 12, x-location within the turbulent flame brush is indicated by the local mean progress variable, $\langle c \rangle$.

Figure 6 shows an instantaneous plot of the spatial variations of the mean flame curvature, $\langle k_m \rangle_S$, through the turbulent flame. The mean curvature goes from positive at the leading edge to negative at the rear edge of the turbulent flame. Since in non-unity Lewis number flames, the local combustion intensity, as measured by the reactant comsumption speed S_C, depends strongly on the flame curvature, and since the dependence is quasi-linear (Haworth & Poinsot 1992, Rutland & Trouvé 1991), it might be inferred from Figure 6 that the statistical distribution of S_C is non-homogeneous as well. Figure 7 shows that this is indeed the case. For $Le < 1$, $\langle S_C \rangle_S$ is a decreasing function of the mean progress variable, $\langle c \rangle$: the combustion intensity is higher at the leading edge than at the rear edge of the turbulent flame. For $Le > 1$, the trends are opposite: the combustion intensity is lower at the leading edge, close to $\langle c \rangle = 0$, than at the rear edge, close to $\langle c \rangle = 1$. For $Le = 1$, $\langle S_C \rangle_S$ remains approximately constant and equal to the laminar flame speed, s_L.

In the flamelet regime, a flame element can be characterized by two speeds: S_C, which is a chemical rate, and w, which is a kinematic quantity and gives the velocity of the flame front with respect to the flow field (Eq.(15)). For a strain-free, plane laminar flame these two speeds are the same and equal to s_L. As pointed out by Poinsot *et al.* (1992), in the context of highly stretched flames, S_C and w can be significantly different. Figure 8 shows the variations of the mean flame propagation speed, $\langle w \rangle_S$, through the turbulent flame. $\langle w \rangle_S$ is an increasing function of the mean progress variable, $\langle c \rangle$. Comparison of Figures 7 and 8 indicate that, for $Le = 0.8$, the leading edge of the turbulent flame burns faster but propagates more slowly than the rear edge of the flame, which burns more slowly but propagates faster into the reactants.

It is worth emphasizing that the dynamical properties of the turbulent flame are not completely described by the knowledge of the distribution of the propagation speed, w, along the flame. To determine whether the flame surface will actually grow or contract, some information about the hydrodynamic flow field has to be included.† In other words, one needs to solve for the Σ-equation.

We now turn to the terms appearing on the right-hand side of the equation for Σ. While the strain term, $\langle a_T \rangle_S$, remains approximately constant through the turbulent flame (Figure 9), the propagation term, $2\langle w k_m \rangle_S$, exhibits strong variations and decreases from positive values on the unburnt side, close to $\langle c \rangle = 0$, to negative values on the burnt side, close to $\langle c \rangle = 1$ (Figure 10). The net effect on the surface growth rate is given by the flame stretch, $\langle k \rangle_S = \langle a_T \rangle_S + 2 \langle w k_m \rangle_S$. Figures 9 and 10 indicate that both contributions to stretch have the same order of magnitude.

† This is best seen in the context of laminar flame instabilities, where the classical linear theory shows that the stability problem is not solved at the level of determining the Markstein length but also requires solving for a dispersion relation, which includes hydrodynamic effects (Clavin 1985, Williams 1985)

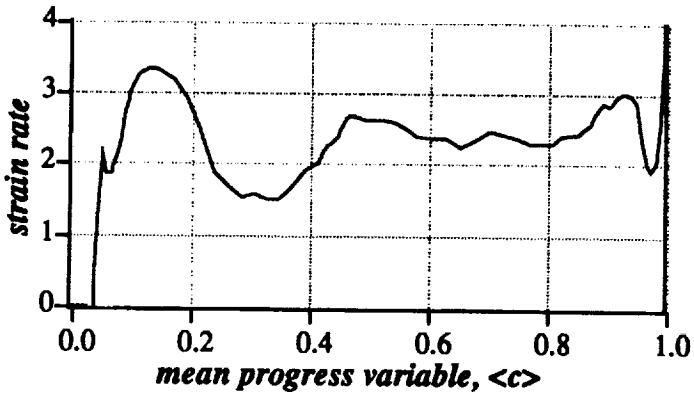

FIGURE 9. Variations of the mean strain rate, $\langle a_T \rangle_S$, through the turbulent flame brush. $Le = 0.8$, $t = 4\ \tau$. Strain rate is made non-dimensional by the characteristic flame time, δ_T / s_L.

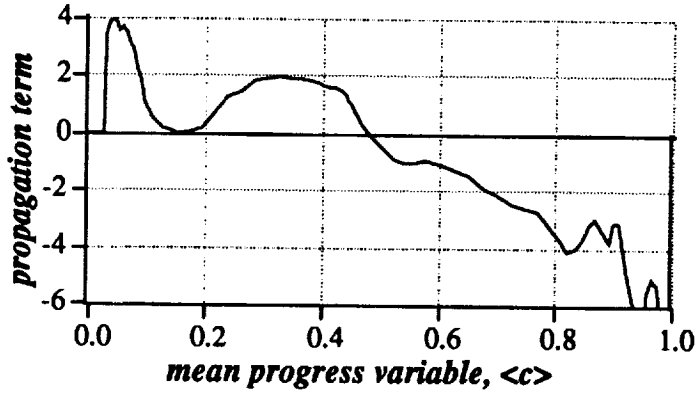

FIGURE 10. Variations of the mean propagation term, $2\langle w k_m \rangle_S$, through the turbulent flame brush. $Le = 0.8$, $t = 4\ \tau$. wk_m is made non-dimensional by the characteristic flame time, δ_T / s_L.

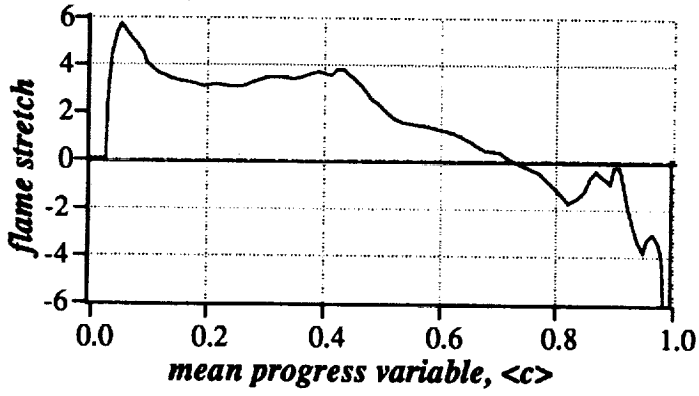

FIGURE 11. Variations of the mean flame stretch, $\langle k \rangle_S$, through the turbulent flame brush. $Le = 0.8$, $t = 4\ \tau$. k is made non-dimensional by the characteristic flame time, δ_T / s_L.

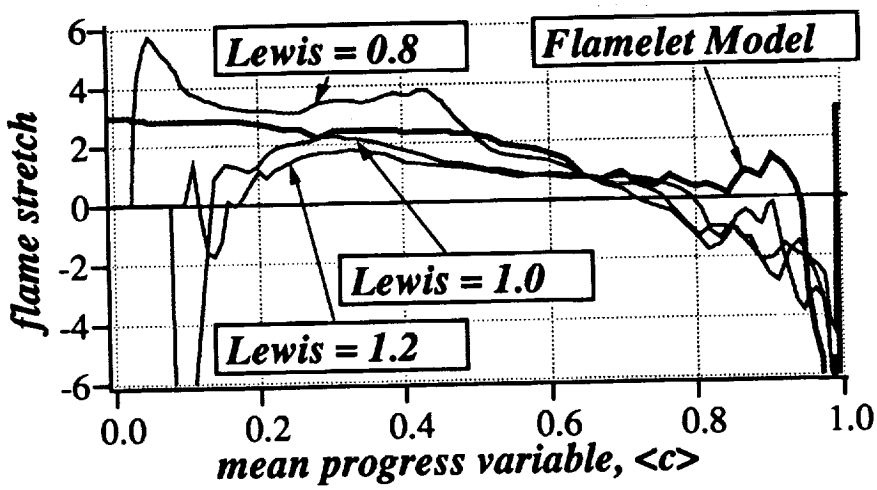

FIGURE 12. Lewis number effects on the variations of the mean flame stretch, $\langle k \rangle_S$, through the turbulent flame brush, and comparison with flamelet models. $t = 4\ \tau$. k is made non-dimensional by the laminar flame time, δ_T / s_L.

Figure 11 presents the mean flame stretch profile through the turbulent reaction zone. At the leading edge, strain rate and flame propagation effects are locally cumulative and the overall balance is strongly positive. The leading edge of the turbulent flame is a region of strong production of flame surface area. On the contrary, the propagation term takes large negative values on the burnt side. In that region, strain rate and flame propagation effects are locally opposite, and the overall balance is negative. The rear edge of the turbulent flame thus appears as a region where flame surface area gets strongly dissipated.

Figure 11 spatially resolves the balance between production and dissipation of flame surface area. The net effect is given by defining a mean stretch, $\overline{k}$, space-averaged throughout the flame brush:

$$\overline{k} = \frac{d}{dt}\left(\frac{S_V(t)}{L_y L_z}\right) = \int \langle k \rangle_S \Sigma \, dx \tag{24}$$

$\overline{k}$ gives the instantaneous rate of change of the flame surface area in the computational domain. If $\overline{k}$ is positive, the flame surface grows; if negative, the flame surface contracts. The next section further discusses the effect of the Lewis number on the spatially-resolved flame stretch profile, as well as the resulting impact on the net mean flame stretch, $\overline{k}$, and presents some comparison with flamelet models.

3.3. Comparison of DNS results with flamelet models

Figure 12 compares the mean flame stretch profiles, $\langle k \rangle_S$, plotted for different Lewis numbers. In all cases, stretch takes large negative values on the burnt side, close to $\langle c \rangle = 1$. The effect of the Lewis number is not visible in that region. On the contrary, at the leading edge of the flame, there are large differences between

the different Lewis number cases. This suggests that the turbulent flame is most sensitive to Lewis number effects on the unburnt side, whereas it remains unaffected on the burnt side. Using Eq. (24), we can quantify the overall differences previously observed in Figure 4; we find (in units of the laminar flame time): $\overline{k} = 2.6$ for $Le = 0.8$, and the flame surface area is quickly growing; $\overline{k} \simeq 0.0$ for $Le = 1.0$ and $Le = 1.2$, and the flame surface area remains roughly constant.

Also plotted in Figure 12 is a comparison with flamelet models. Many current flamelet models use a transport equation for the flame surface density. Different formulations of this equation have been proposed in the literature (Marble & Broadwell 1977, Candel *et al.* 1990, Cant *et al.* 1990, Borghi 1990). For the sake of comparison, we use a closure assumption similar to the one proposed in the Coherent Flame Model by Marble & Broadwell (1977) and Candel *et al.* (1990). In this formulation, the turbulent flame stretch is written as:

$$k = \frac{\epsilon}{k_t} - s_L \frac{\Sigma}{\langle Y_R \rangle}, \tag{25}$$

where k_t is the turbulent kinetic energy and ϵ its dissipation; $\langle Y_R \rangle$ is the ensemble-averaged fuel mass fraction. The first term on the right-hand side of Eq.(25) represents straining due to the flow motions and is assumed to scale with the integral time scale of the turbulence; the second term is a disparition term associated with flame propagation and is assumed to scale with the laminar flame speed, s_L, and the flame surface density, Σ.

Figure 12 shows that this model is indeed able to reproduce qualitatively the spatial structure of the balance between production and dissipation of Σ, going from production at the leading edge of the turbulent flame to dissipation at the rear edge. However, the $1/\langle Y_R \rangle$ behavior of the disparition term leads to numerical difficulties on the burnt side of the flame. The model, therefore, overpredicts the dissipation of Σ, near $\langle c \rangle = 1$, and gives a negative mean flame stretch, $\overline{k} = -3.6$, in strong disagreement with the values reported above. In addition, the disparition term in Eq.(25) is always and everywhere negative and cannot account for the possible transition to unstable flame conditions as observed in the simulations.

4. Conclusion

Flamelet models constitute one of the most common approach for turbulent premixed combustion. In these models, the flame surface density is a central ingredient that conveys most of the effects of the turbulence on the rate of energy release. The flame surface density is usually obtained via a modeled transport equation, called the Σ-equation, first postulated by Marble & Broadwell (1977). Recent theoretical work, based on conservation equations for surfaces and volumes in a turbulent flow field, has produced a more rigorous approach that leads to an exact, but unclosed, formulation for the turbulent Σ-equation (Pope 1988, Candel & Poinsot 1990). In this exact Σ-equation, it appears that the dynamical properties of the flame surface density are determined by a single parameter, namely the turbulent flame stretch. Unfortunately, the flame surface density and the turbulent flame stretch

are extremely difficult to measure and are simply not available from experiments. Therefore, little is known on the validity of the closure assumptions used in current formulations of flamelet models.

Direct Numerical Simulation (DNS) is the obvious, complementary approach to get basic information on these fundamental quantities. In the present work, three-dimensional DNS of premixed flames propagating in isotropic turbulent flow have been used to estimate the different terms appearing in the Σ-equation. A new methodology has been proposed to provide the source and sink terms for the flame surface density, estimated as a function of time and position within the turbulent flame brush. Using this methodology, the effects of the Lewis number on the rate of production of flame surface area are described in great detail. Principal findings are that: (1) the balance between production and dissipation of flame surface area is strongly non-homogeneous: the leading edge of the turbulent flame is a region of production of flame surface area, whereas the rear edge is a region where flame surface gets strongly dissipated; (2) the turbulent flame is most sensitive to Lewis number effects at the leading edge, whereas it remains unaffected on the burnt side. These results suggest that most of the important dynamical features of turbulent flames take place at the leading edge of the reaction zone.

Detailed comparisons with flamelet models were also performed. The analysis reveals the tendency of the models to overpredict flame surface dissipation as well as their inability to reproduce variations due to thermo-diffusive phenomena. Thanks to the detailed information produced by a DNS-based analysis, this type of comparison not only underscores the shortcomings of current models but also suggests ways to improve them. Future work will focus on the development of a new formulation of the Σ-equation that would incorporate thermo-diffusive mechanisms.

Acknowledgements

The authors acknowledge the fruitful interaction with other members of the combustion group during the 1992 CTR summer program. In particular, we thank Dr. Feng Gao for his many insights during the program. We also thank Prof. Stephen Pope and Prof. Forman Williams for their helpful comments and suggestions.

REFERENCES

ABDEL-GAYED, R. G., BRADLEY, D., HAMID, M. N., & LAWES, M. 1984 Lewis number effects on turbulent burning velocity. *Twentieth Symp. (International) on Combust.* 505-512. The Combustion Institute.

ASHURST, W. T., PETERS, N., & SMOOKE, M. D. 1987 Numerical simulation of turbulent flame structure with non-unity Lewis number. *Combust. Sci. Technol.* **53,** 339-375.

BARRÈRE, M. 1974 Modèles de combustion turbulente. *Revue Générale de Thermique.* **148,** 295-308.

BORGHI, R. 1985 On the structure and morphology of turbulent premixed flames. *in Recent Advances in Aerospace Sciences.* Pergamon.

BORGHI, R. 1990 Turbulent premixed combustion: further discussion on the scales of the fluctuations. *Combust. Flame.* **80,** 304-312.

BRAY, K. N. C 1980 Turbulent flows with premixed reactants. *in Topics in Applied Physics* **44.** Springer-Verlag.

CANDEL, S. M., VEYNANTE, D., LACAS, F., MAISTRET, E., DARABIHA, N., & POINSOT, T. 1990 Coherent flame model: applications and recent extensions. *in Series on Advances in Mathematics for Applied Sciences.* World Scientific.

CANDEL, S. M., & POINSOT, T. 1990 Flame stretch and the balance equation for the flame surface area. *Combust. Sci. Technol.* **70,** 1-15.

CLAVIN, P., & GARCIA, P. 1983 The influence of temperature dependence of diffusivities on the dynamics of flame fronts. *J. Mécanique.* **2,** 245-263.

CLAVIN, P. 1985 Dynamic behavior of premixed flame fronts in laminar and turbulent flows. *Prog. Energy Combust. Sci.* **11,** 1-59.

CANT, R. S., POPE, S. B., & BRAY, K. N. C. 1990 Modelling of flamelet surface-to-volume ratio in turbulent premixed combustion. *Twenty-Third Symp. (International) on Combust.* 809-815. The Combustion Institute.

GOIX, P. J., & SHEPERD, I. G. 1992 Lewis number effects on turbulent premixed flame structure. *Fall Meeting of the Western States Section.* The Combustion Institute.

HAWORTH, D. C., & POINSOT, T. 1992 Numerical simulations of Lewis number effects in turbulent premixed flames. *J. Fluid Mech.* **244,** 405-436.

LELE, S. K. 1990 Compact finite difference schemes with spectral-like resolution. *J. Comp. Phys.* (submitted for publication).

MARBLE, F. E., & BROADWELL, J. E. 1977 The coherent flame model for turbulent chemical reactions. *Project Squid Technical Report.* TRW-9-PU.

PETERS, N. 1986 Laminar flamelet concepts in turbulent combustion. *Twenty-First Symp. (International) on Combust.* 1231-1250. The Combustion Institute.

POINSOT, T., VEYNANTE, D., & CANDEL, S. M. 1991 Quenching processes and premixed turbulent combustion diagrams. *J. Fluid Mech.* **228,** 561-605.

POINSOT, T., ECHEKKI, T., & MUNGAL, M. G. 1992 A study of the laminar flame tip and implications for premixed turbulent combustion. *Combust. Sci. Technol.* **81,** 45-73.

POINSOT, T., & LELE, S.K. 1992 Boundary conditions for direct simulations of compressible viscous flows.. *J. Comp. Phys.* **101,** 104-129.

POPE, S. B. 1988 Evolution of surfaces in turbulence. *International J. Engng. Sci.* **26,** 445-469.

POPE, S. B. 1990 Computations of turbulent combustion: progress and challenges. *Twenty-Third Symp. (International) on Combust.* The Combustion Institute.

RUTLAND, C. J., & TROUVÉ, A. 1991 Direct simulations of premixed turbulent flames with non-unity Lewis numbers. *Combust. Flame* (submitted for publication).

WU, M. S., KWON, S., DRISCOLL, J. F., & FAETH, G. M. 1990 Turbulent premixed hydrogen/air flames at high reynolds numbers. *Combust. Sci. Technol.* **73**, 327-350.

WILLIAMS, F. A. 1985 *Combustion theory.* 2nd ed., Benjamin Cummings.

WRAY, A. A. 1990 Minimal storage time-advancement schemes for spectral methods. *J. Comp. Phys.* (submitted for publication).